

Supporting information

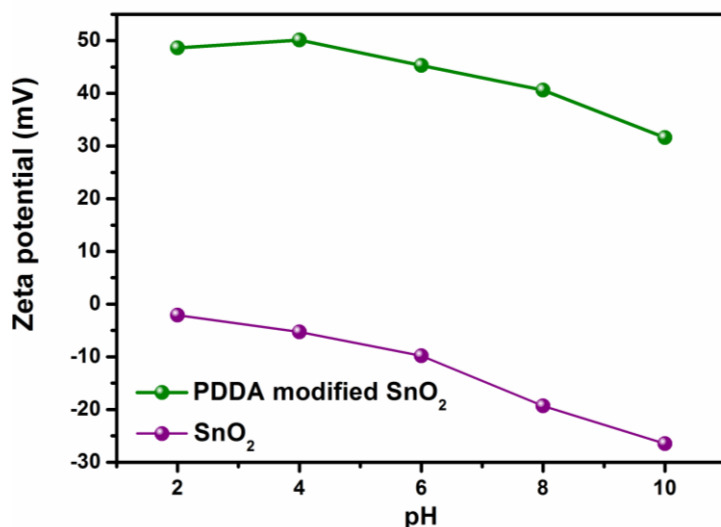


Fig. S1 Zeta potential of  $\text{SnO}_2$  and PDDA modified  $\text{SnO}_2$  in solution at different pH values

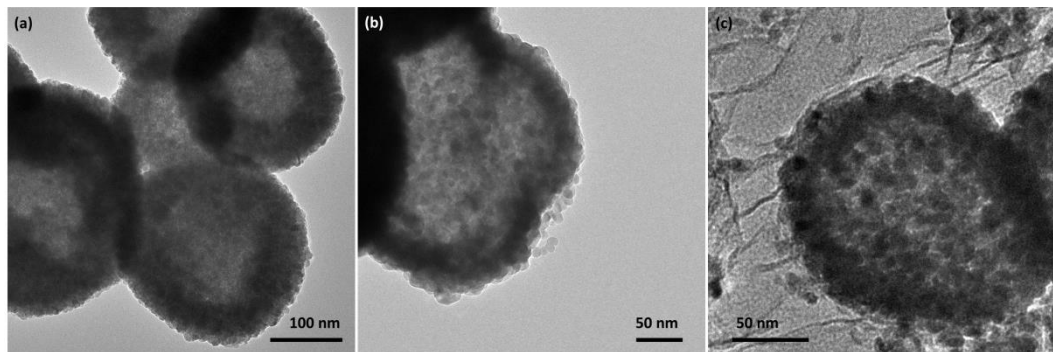


Fig. S2 TEM images of (a)  $\text{SnO}_2$ , (b)  $\text{SnO}_2/\text{C}$  and (c)  $\text{SnO}_{2-x}/\text{N-rGO}$

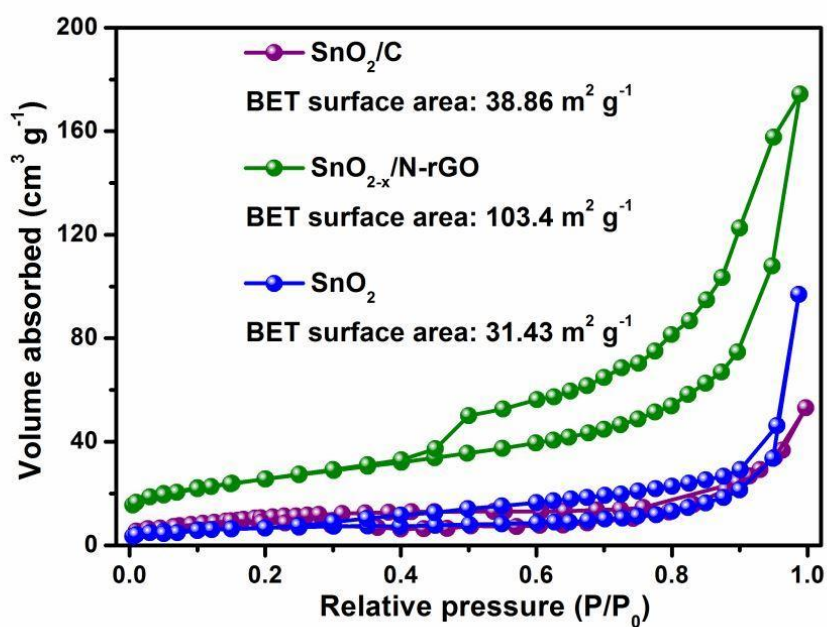


Fig. S3  $\text{N}_2$  adsorption/desorption isotherms of the  $\text{SnO}_2$ ,  $\text{SnO}_2/\text{C}$  and  $\text{SnO}_{2-x}/\text{N-rGO}$

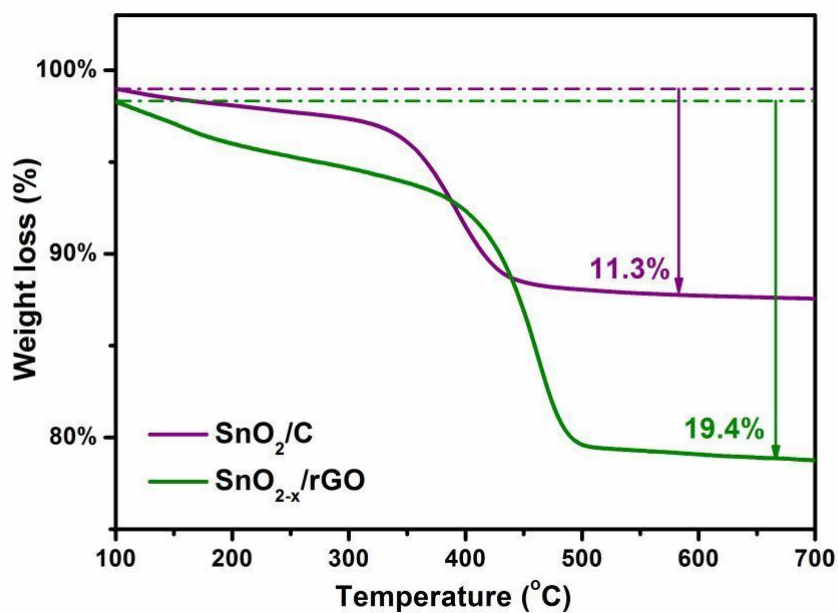


Fig. S4 TG curves of  $\text{SnO}_2/\text{C}$  and  $\text{SnO}_{2-x}/\text{N-rGO}$  samples

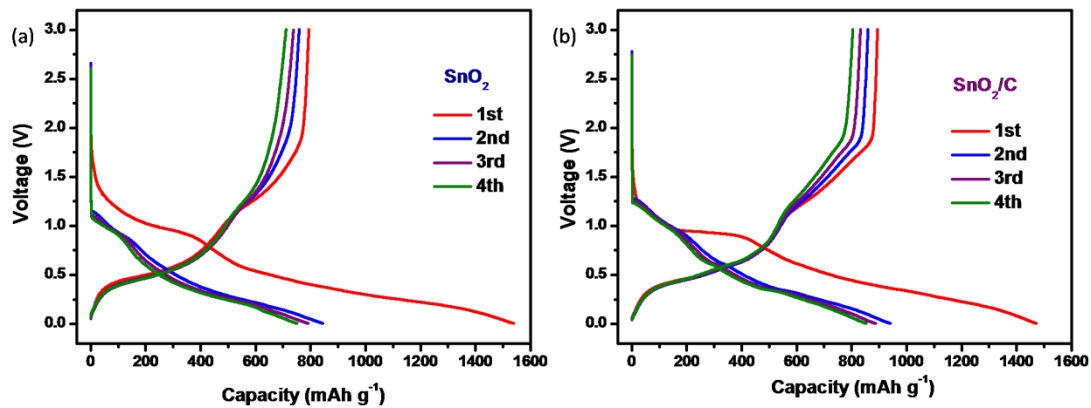


Fig. S5 The first four discharge-charge curves of (a)  $\text{SnO}_2$  and (b)  $\text{SnO}_2/\text{C}$  electrode at a current density of  $0.1 \text{ A g}^{-1}$

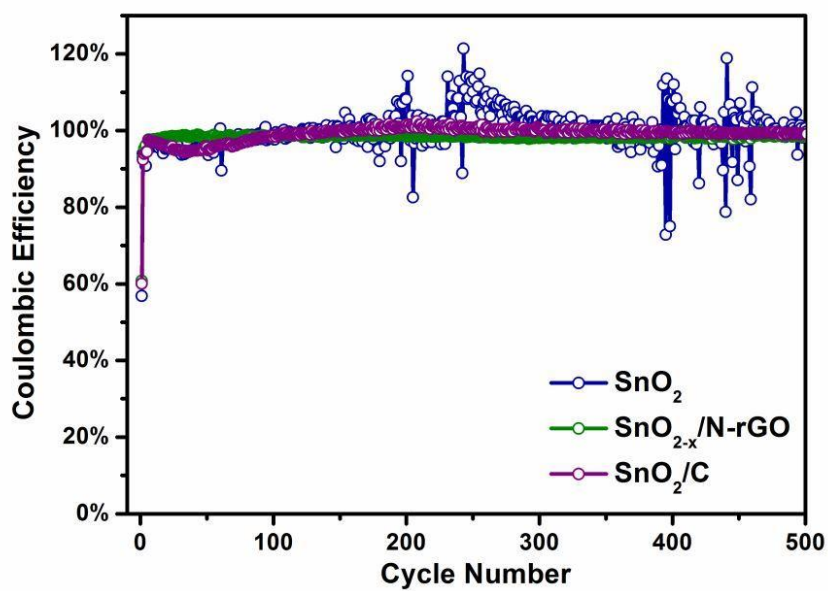


Fig. S6 Coulombic efficiency curves of as-prepared  $\text{SnO}_2$  samples under  $0.5 \text{ A g}^{-1}$

Table S1 Cyclic performance comparison of as-prepared SnO<sub>2</sub>/rGO with previous work about SnO<sub>2</sub>/graphene-based anode materials

Material	Cycle number	Current density (A g <sup>-1</sup> )	Specific capacity retention (mAh g <sup>-1</sup> )	Reference
SnO <sub>2</sub> /rGO	500	1.0	552	<i>J. Mater. Chem. A</i> , 2017, 5, 4535-4542
SnO <sub>2</sub> /graphene@C	100	0.1	820	<i>J. Mater. Chem. A</i> , 2016, 4, 362-367
SnO <sub>2</sub> @graphene/ Pani	100	0.1	770	<i>ACS Appl. Mater. Interfaces</i> , 2015, 7, 2444-2451
SnO <sub>2</sub> /rGO/C foam	100	0.13	717	<i>ChemElectroChem</i> , 2016, 3, 1063-1071
SnO <sub>2</sub> /rGO	100	0.1	536	<i>Electrochimica Acta</i> , 2016, 207, 9-15
SnO <sub>2</sub> quantum dots@GO	100	0.1	1121	<i>Small</i> , 2016, 12, 588-594
SnO <sub>2</sub> @polyaniline @graphene	100	1.0	560	<i>J. Power. Sources</i> , 2015, 290, 61-70
SnO <sub>2</sub> /C/graphene sheets	100	0.2	830	<i>ACS Appl. Mater. Interfaces</i> , 2014, 6, 7434-7443
SnO <sub>2</sub> @double graphene	120	0.08	591	<i>Nano Energy</i> , 2014, 3, 80-87
SnO <sub>2</sub> /GO composite	200	0.1	800	<i>J. Mater. Chem. A</i> , 2013, 1, 7558-7562
SnO <sub>2</sub> /graphene nanobelts	50	0.1	825	<i>ACS Nano</i> , 2013, 7, 6001-6006
SnO <sub>2</sub> /graphene composite	200	0.1	830	<i>Adv. Mater.</i> 2013, 25, 3307-3312
Mesoporous SnO <sub>2</sub> @graphene	50	0.078	848	<i>Adv. Funct. Mater.</i> , 2013, 23, 3570-3576
SnO <sub>2</sub> with oxygen vacancies wrapped in N-doped rGO	500	0.5	912	<b>Our work</b>

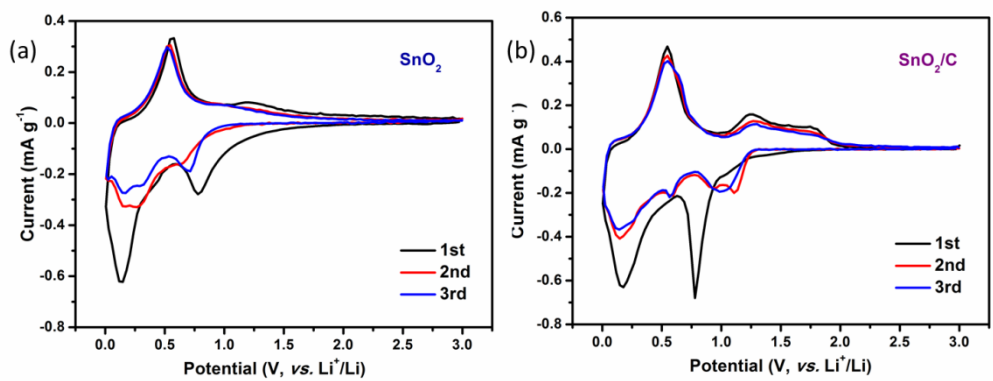


Fig. S7 CV curves of (a)  $\text{SnO}_2$  and (b)  $\text{SnO}_2/\text{C}$  electrode in the voltage of 0.005 to 3.0 V at a scanning rate of  $0.1 \text{ mV s}^{-1}$

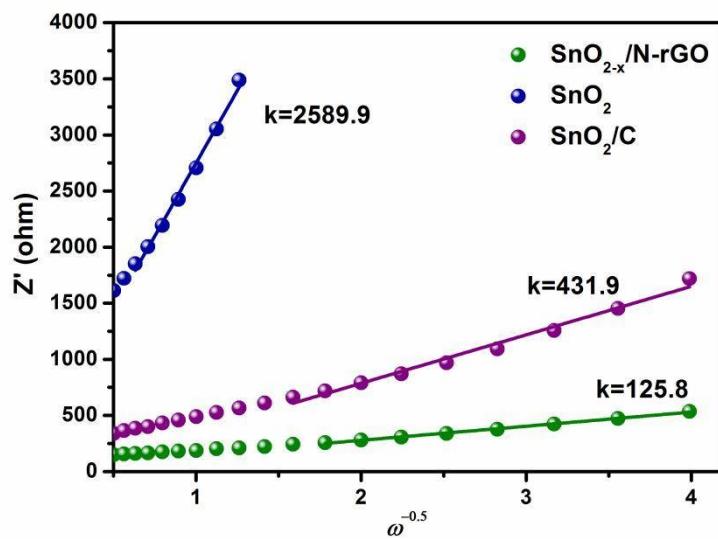


Fig. S8 The relationship between  $Z'$  and  $\omega^{-0.5}$  of as-prepared  $\text{SnO}_2$  samples

Table S2 The values of  $R_f$ ,  $R_{ct}$  and  $D_{Li}$  calculated from the Nyquist plots

	$R_s$ ( $\Omega$ )	$R_{ct}$ ( $\Omega$ )	$\sigma$
$\text{SnO}_2$	20.3	534.4	2589.9
$\text{SnO}_2/\text{C}$	19.5	124.6	431.9
$\text{SnO}_{2-x}/\text{N-rGO}$	6.1	55.7	125.8

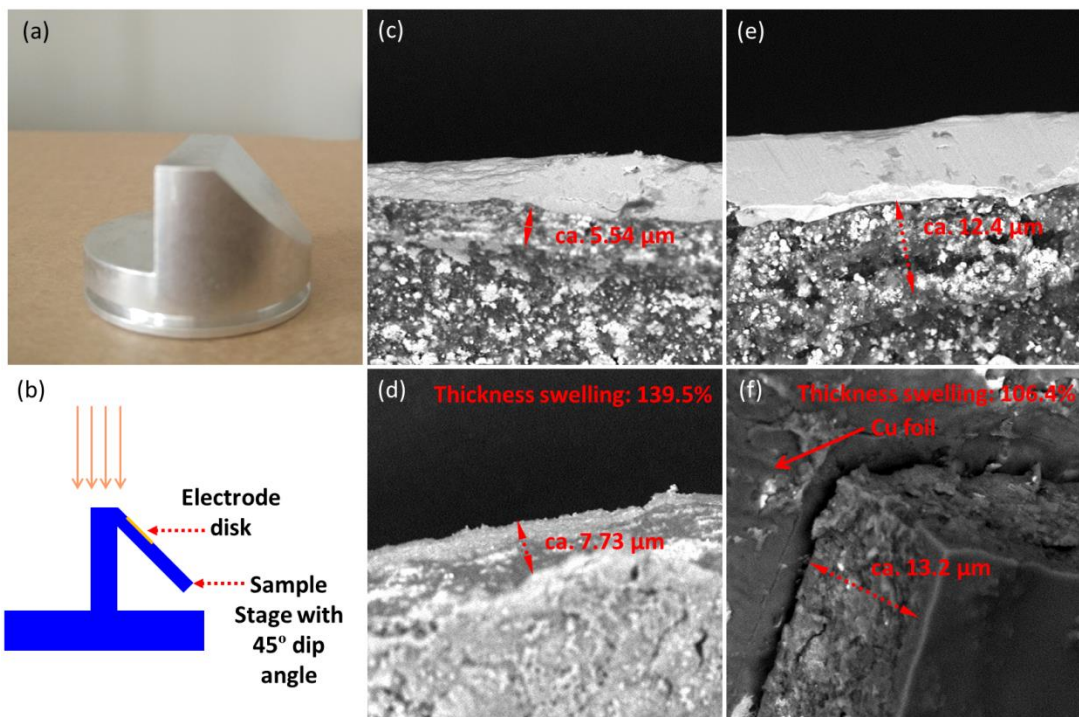


Fig. S9 (a) Photo of the sample stage; (b) working schematic of the sample stage with dip angle; SEM images of  $\text{SnO}_2$  electrode disk (c) at initial status and (d) after cycles, and  $\text{SnO}_{2-x}/\text{N-rGO}$  electrode disk (e) at initial status and (f) after cycles.